

Supplemental Material to:

**Ekaterina S Gushchanskaya, Artem V Artemov,
Sergey V Ulyanov, Maria D Logacheva, Aleksey A Penin,
Elena S Kotova, Sergey B Akopov, Lev G Nikolaev,
Olga V Iarovaia Eugene D Sverdlov, Alexey A Gavrilov,
and Sergey V Razin**

**The clustering of CpG islands may constitute an important
determinant of the 3D organization of interphase
chromosomes**

Epigenetics 2014; 9(7)

<http://dx.doi.org/10.4161/epi.28794>

**[http://www.landesbioscience.com/journals/epigenetics/
article/28794/](http://www.landesbioscience.com/journals/epigenetics/article/28794/)**

SUPPLEMENTARY TABLES

Table S1. The reference bait-originated subsequences for the 4C anchors. These sequences appeared at the beginning of the 4C reads before the *Hind*III restriction sites and originated from the anchor DNA fragments. The sequences were trimmed (see Material and Methods).

| Anchor | Reference sequence |
|----------|--|
| TSR3 | CACTCATCTCCCCGTA CTTTGCCCTAATTCCTCAAGCTT |
| GENE-Des | AATTTGTGAAGCAGTTGTATGTAGTCAGCAACAGAAGTACAAGCTT |
| NPRL3 | GCCAGGATATAGATTCTGCTTTTAAGCTT |
| TRAP1 | CCAGAGATTCTCAAATCACAGCACAGAAGCTT |
| PPL | AAAGCATCTCCTCTCCCTGAAGAGCAGAGAGCGGCTCCAAAGCTT |

SUPPLEMENTARY FIGURE LEGENDS

Figure S1. Scatterplots and box-plots showing the relationships between the TSR3 4C signal (y-axis) in HD3 cells and the densities of various genomic features (x-axis). (A-G) The correlation of the TSR3 4C signal with the CGI density (A), Sp1 motifs (B), CTCF motifs (C), CTCF deposition sites, as determined by ChIP-Seq (D), NF-E2 binding motifs (E), GATA1 binding motifs (F), and G-quadruplex motifs (G) is shown. Other designations are as in Figure 3.

Figure S2. Scatterplots and box-plots showing the relationships between the GENE-Des 4C signal (y-axis) in HD3 cells and the densities of various genomic features (x-axis). (A-G) The correlation of the GENE-Des 4C signal with the CGI density (A), Sp1 motifs (B), CTCF motifs (C), CTCF deposition sites, as determined by ChIP-Seq (D), NF-E2 binding motifs (E), GATA1 binding motifs (F), and G-quadruplex motifs (G) is shown. Other designations are as in Figure 3.

Figure S3. Scatterplots and box-plots showing the relationships between the TRAP1 4C signal (y-axis) in HD3 cells and the densities of various genomic features (x-axis). (A-G) The correlation of the TRAP1 4C signal with the CGI density (A), Sp1 motifs (B), CTCF motifs (C),

CTCF deposition sites, as determined by ChIP-Seq (D), NF-E2 binding motifs (E), GATA1 binding motifs (F), and G-quadruplex motifs (G) is shown. Other designations are as in Figure 3.

Figure S4. Scatterplots and box-plots showing the relationships between the PPL 4C signal (y-axis) in HD3 cells and the densities of various genomic features (x-axis). (A-G) The correlation of the PPL 4C signal with the CGI density (A), Sp1 motifs (B), CTCF motifs (C), CTCF deposition sites, as determined by ChIP-Seq (D), NF-E2 binding motifs (E), GATA1 binding motifs (F), and G-quadruplex motifs (G) is shown. Other designations are as in Figure 3.

Figure S5. Distribution of the CTCF deposition sites in the upstream area of the chicken c-myc gene. The figure demonstrates the position of the CTCF binding site reported by Lobanenkov et al (site V)⁷⁸ and CTCF binding sites found in our ChIP-Seq experiments (shown are the raw data of the ChIP-Seq analysis and CTCF deposition peaks identified as described in Material and Methods); visualization in the UCSC browser. Genomic coordinates are according to the galGal4 assembly.

SUPPLEMENTARY FIGURES

Figure S1

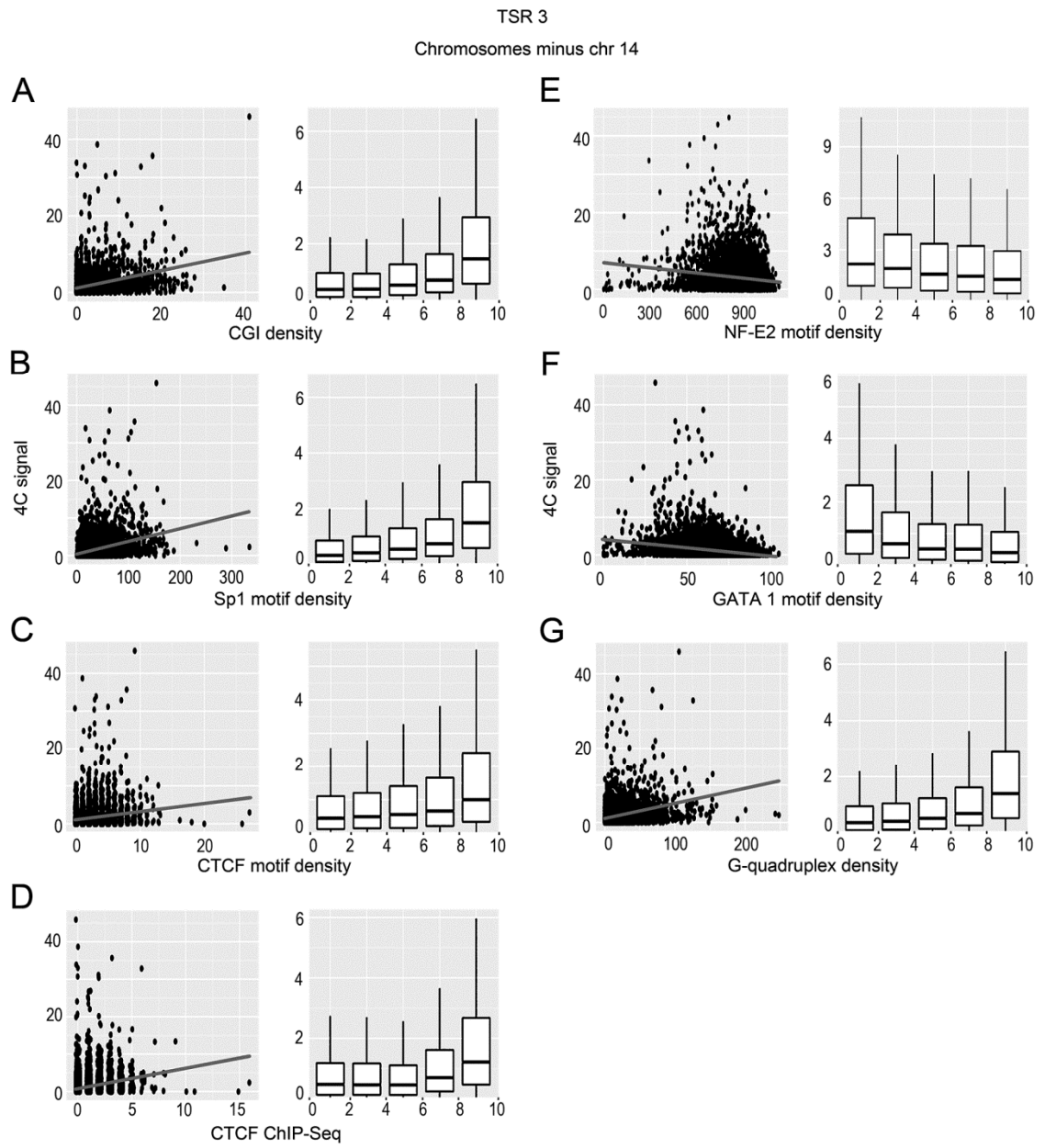


Figure S2

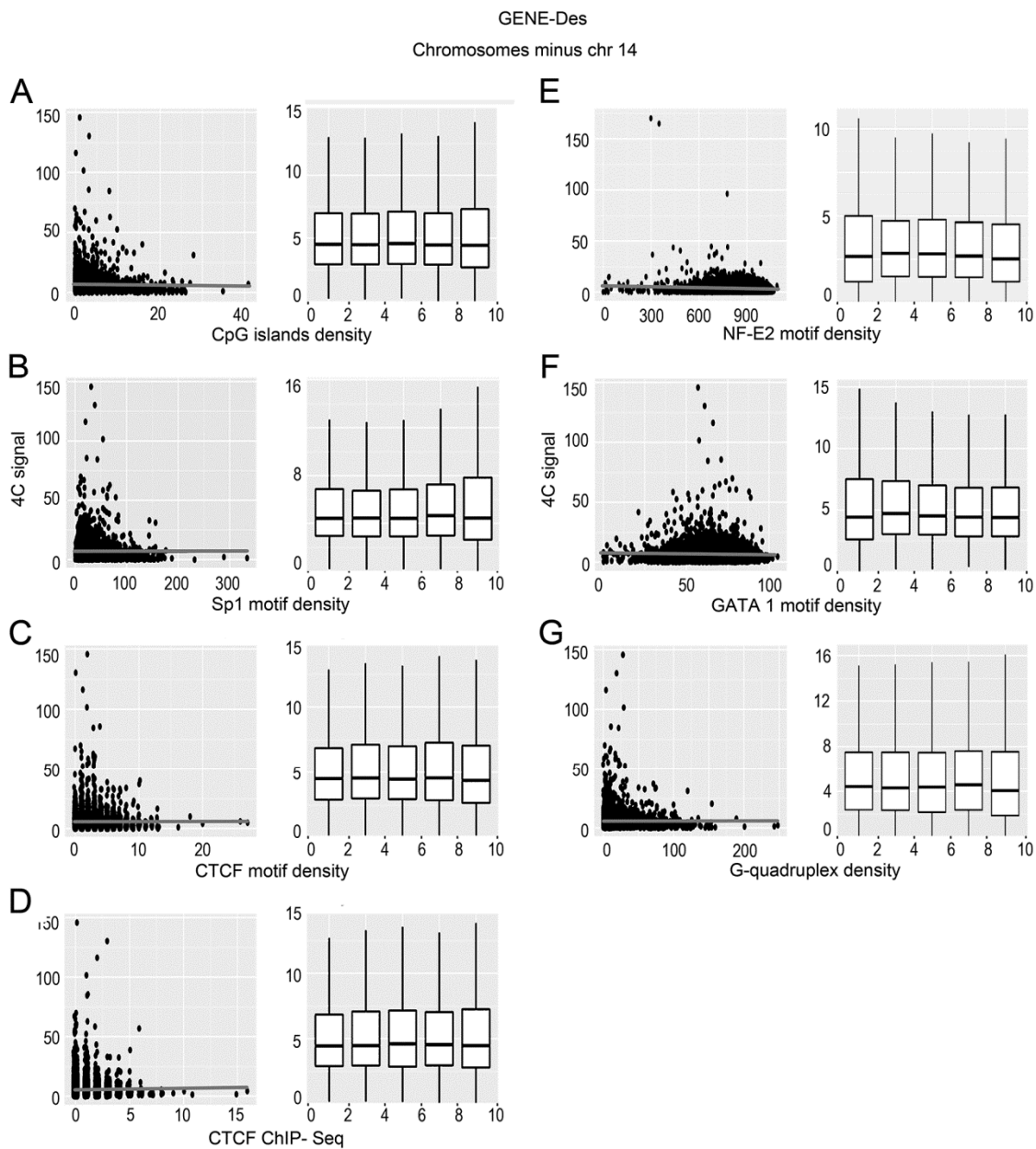


Figure S3

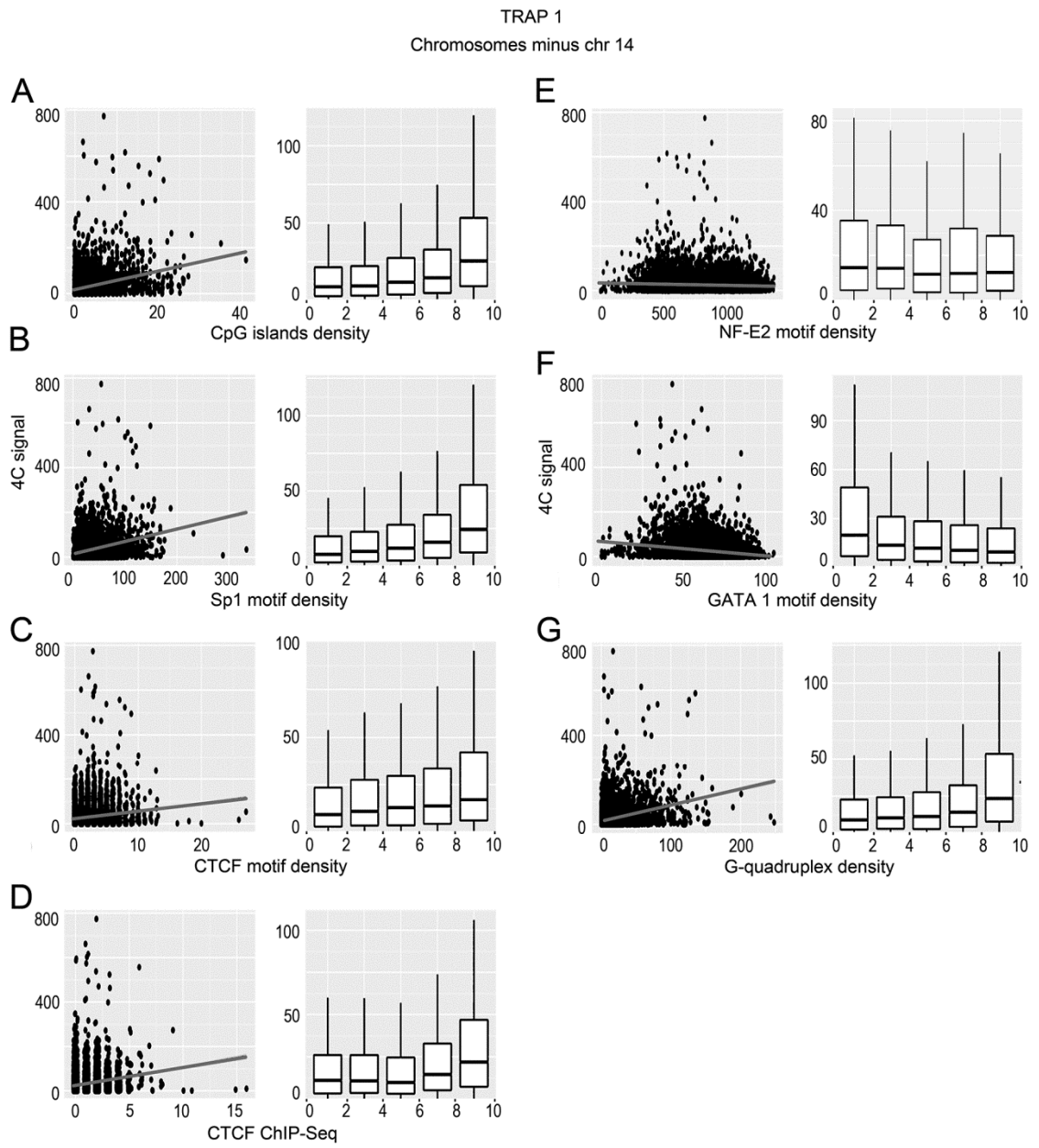


Figure S4

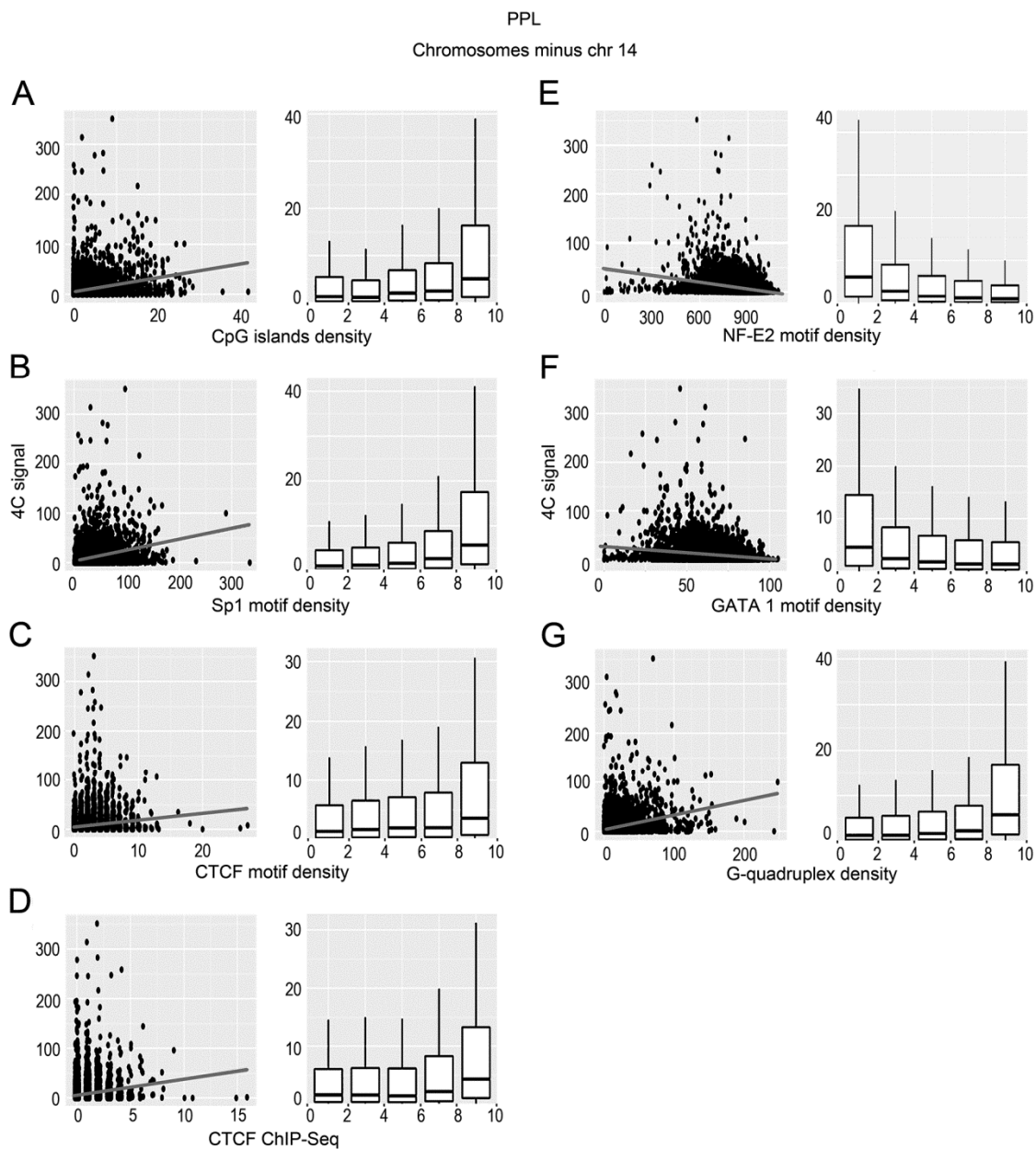


Figure S5

